

# FUNCTIONALIZED INORGANIC NANOSTRUCTURES FOR BIOMEDICAL APPLICATIONS

Bonroy K. \*, Jans H.\*<sup>§</sup>, Van de Broek B.\*<sup>§</sup>, Jans K.\*<sup>§</sup>, Reekmans G. \*, Van Summeren A. \*, Van Meerbergen B. \*, Huang C. \*, Stakenborg T. \*, Trekker J.\*<sup>#</sup>, Willems M. \*, Bartic C. \*, Verhaegen K. \* and Borghs G.\*

\*IMEC, NEXT, Kapeldreef 75, 3001 Heverlee, Belgium, bonroyk@imec.be

<sup>§</sup>K.U. Leuven, Department of Chemistry, Celestijnenlaan 200F, 3001 Heverlee, Belgium

<sup>#</sup> K.U. Leuven, Biomedical Science, Radiology, O&N I Herestraat 49, 3000 Leuven, Belgium

## ABSTRACT

Nanomaterials differ significantly from other materials due to two factors: increased surface area and quantum size effects. These factors can enhance properties such as reactivity, strength and physical characteristics. Due to these properties, the coupling of nanomaterials to biomolecular entities has the potential to revolutionize many fields of science and technology.

Our main goal is to synthesize tunable functionalized nanostructures and to explore their use in applications such as (bio)sensing, diagnostics, imaging, and treatment. To allow a full exploration, these nanostructures need to be developed at the crossroads of chemistry, biology and engineering. IMEC, one of Europe's leading independent research center in the field of microelectronics and nanotechnology, is carrying out controlled interactions of biomolecules with various nanostructures that might be important for modern bioelectronics and life sciences.

**Keywords:** Inorganic nanoparticles, Functionalization, Biosensing, Hyperthermia, Imaging

## 1 INTRODUCTION

Nanoparticles are very important tools for a number of applications ranging from biomedics to photonics and storage. This has necessitated the continuous search for novel synthesis routes of **inorganic nanoparticles** fabricated from different materials. From the material point of view, these particles are so small that they exhibit characteristics that are often not observed in the bulk materials. For example, gold nanoparticles have unique optical properties such as a strong absorption, while magnetic nanoparticles show remarkable size-related properties such as superparamagnetism. These nanoscaled properties of nanoparticles make them useful for diverse biomedical applications including biosensing, imaging and hyperthermia-based therapy.

**Noble metal nanoparticles** such as Ag and Au have fascinated people since ancient times, and nowadays the interest for these structures is still increasing. The bright colors of the noble metal nanoparticles are the result of the presence of a plasmon absorption band. This band occurs when the frequency of incoming photons is in resonance with the collective excitation of the conducting electrons of the particles. This effect is termed "Localized Surface Plasmon Resonance" (LSPR) [1]. The LSPR properties of the nanoparticles depend on different parameters such as

the size, the shape, the material, the particle-particle interactions and the local environment including substrate, solvent and adsorbates. This phenomenon is the basis of their use in biosensing or hyperthermia applications.

Properties of **magnetic materials** such as blocking temperature, spin life time, coercivity, and susceptibility are strongly influenced when scaling the materials dimension to the nanoscale. By using a controlled nanoscaling in combination with different types of material, it is also possible to tune the above-mentioned magnetic parameters towards the development of novel nanomaterials with superior properties. This tuning of the magnetic parameters is critical for the design of the ideal and optimized characteristics of functionalized magnetic nanoparticles and their enhanced applicability in biomedical applications such as contrast agents for magnetic resonance imaging (MRI).

In this paper, we discuss different synthesis and surface modification methods to obtain stable metal and superparamagnetic nanostructures especially designed for the needs defined by a selection of biological applications including LSPR sensing, hyperthermia and imaging. For all these application a well-characterized chemical and biological functionalization is required and could be advantageous for selectivity or targeting issues.

## 2 FABRICATION OF NANOPARTICLES

### 2.1 Synthesis of gold nanoparticles

The synthesis of **spherical Au nanoparticles** was performed as described previously [2]. Briefly, a first solution consisting of boiling 0.01 % (w/v) HAuCl<sub>4</sub> is prepared and mixed with various amounts of citrate 1% (w/v). The addition of different amounts of citrate to the HAuCl<sub>4</sub> solution results in Au nanoparticles with different sizes ranging from 18-52 nm as confirmed by TEM measurements (Figure 1a). Their absorbance in the UV/Vis spectra showed a maximum band at wavelengths between 518-542 nm.

The synthesis method for the **star shaped gold nanoparticles** is adapted from a previously described procedure [3]. Hereby, 0.4 mg bis(p-sulfonatophenyl) phenylphosphine dihydrate dipotassium and 20 µl hydrogen peroxide (30 %) are mixed with 10 ml of 6.8x10<sup>-3</sup> M sodium citrate. Next, under continuous shaking, 20 µl of 0.05 M HAuCl<sub>4</sub> was slowly added at RT at a flowrate of 10 µl/min. After several minutes, the solution color changed from colorless to blue. The resulting blue colloids can be kept for several days in the refrigerator, although eventually

a blue spectral shift takes place towards red colored particles. The resulted Au nanoparticles have a main diameter of ~50 nm (Figure 1b).

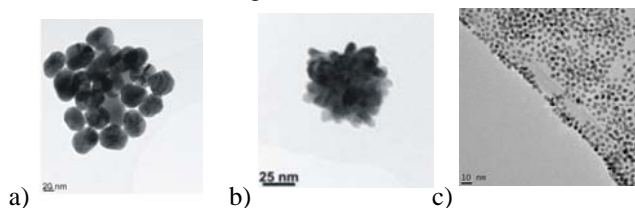


**Figure 1:** TEM images of spherical gold (a) and star shaped gold (b) and FePt (c) nanoparticles.

## 2.2 Fabrication of nanoparticle films

For certain LSPR sensing applications, the synthesized gold nanoparticles are not used in suspension, but they are deposited on a carrier substrate such as quartz or glass. Hereto, the substrates were immersed in a 10 % (v/v) of 3-mercaptopropyltrimethoxysilane in 95 % ethanol: 5 % H<sub>2</sub>O (v/v). After 3 h of silane deposition, the samples were thoroughly rinsed. The cross-linking was promoted in an oven at 110 °C. Immediately after the silanization, the samples were immersed in the nanoparticle suspensions for at least 24 h.

## 2.3 Synthesis of magnetic nanoparticles

There are various reports available that highlight different synthesis approaches for the generation of magnetic nanoparticles. The most common method to generate highly monodisperse nanoparticles is the thermal decomposition method. Fe<sub>3</sub>O<sub>4</sub> as well as FePt nanoparticles were synthesized using this method. The disadvantage of this approach is that the synthesis is performed in organic solvent.

Fe<sub>3</sub>O<sub>4</sub> nanoparticles were synthesized by the reductive thermal decomposition of Fe[acac]<sub>3</sub> through reaction with 1,2-hexadecanediol in the presence of oleic acid and oleylamine as capping agents [4]. While FePt nanoparticles (Figure 1c) were prepared by the simultaneous reductive thermal decomposition of Pt[acac]<sub>2</sub> using 1,2-hexadecanediol and the thermal decomposition of Fe[CO]<sub>5</sub> in the presence of oleic acid and oleylamine as capping agents [5].

## 3 FUNCTIONALIZATION OF INORGANIC NANOPARTICLES

In all biomedical applications it is of utmost importance that the nanoparticles are water-dispersible and capable of surviving in complex environments especially electrolytic environments. Maintaining the colloidal stability for a long time period without aggregation is an important study. A straightforward way to achieve colloidal stability and biocompatibility is the modification of the nanoparticles surface with a suitable capping agent (chemical modification). The stabilized colloids can also be further

modified with biological molecules such as antibodies or peptides.

### 3.1 Functionalization of gold nanoparticles in suspension

The spherical and star shaped gold nanoparticles were chemically modified with suitable self-assembled monolayers of thiols bearing poly(ethylene-oxide) units (PEO). The functionalization method is based on a previously reported protocol [6]. Briefly, the gold colloids were first adjusted to pH 11 by adding dropwise NaOH (0.5 M). The thiols (10 mM) of interest are added to the colloidal mixture in a molar ratio 10:1. Subsequently, the colloid is stirred for at least 3 h to provide sufficient time to build up densely packed monolayers on the nanoparticle surface. To remove the excess of free thiols the gold nanoparticles are washed a few times by centrifugation, followed by decantation of the supernatans and resuspension of the pellet in water.

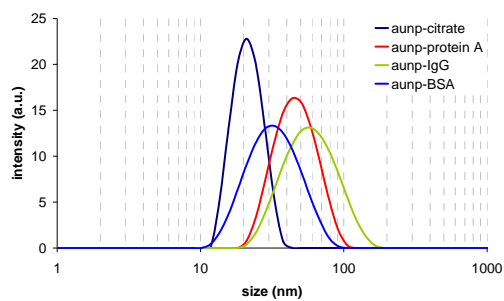


**Figure 2:** DLS spectra of different functionalized gold nanoparticles (citrate nanoparticles versus nanoparticles coated with protein A, IgG and BSA).

Besides chemical modification, the selected biological applications also require attachment of biological molecules (such as antibodies) onto the outer surface of the nanoparticles. Hereto the pH of the nanoparticle suspension is first adjusted to 0.5 units above the pI of the protein of interest using 0.01 M Na<sub>2</sub>CO<sub>3</sub>. Subsequently, the protein solution is added to the gold colloid with a final concentration of 20 µg/mL using continuous shaking. The colloid is further stabilized with a BSA blocking solution with a final concentration of ~0.5 %. The mixture is left for 15 min on a shaking device. To remove the excess of proteins, the colloidal solution is centrifuged gently at a speed of 3000 rpm followed by a resuspension of the functionalized nanoparticles in a suitable buffer solution. The functionalized nanoparticles are characterized using dynamic light scattering (DLS) (Figure 2). The hydrodynamic radius of the nanoparticles clearly increases after modification of the nanoparticles with different proteins.

### 3.2 Functionalization of gold nanoparticle films

To allow biofunctionalization of the nanoparticle films, the particles were first modified with self-assembled

monolayers of thiols. Hereto, the freshly prepared nanoparticle films were immersed for 1 h in a 1 mM mercaptohexadecanoic acid solution in ethanol. After the SAM deposition, the thiol-coated nanoparticle films were further modified using a mixture of 0.4 M EDC and 0.1 M NHS. After 15 minutes of activation, the desired receptor molecules are covalently attached on the activated surface using a suitable coupling buffer. Blocking of the surface was performed using 1 M ethanolamine.

### 3.3 Functionalization of magnetic nanoparticle

The phase transfer of magnetic nanoparticles from an organic solvent to water was performed through reaction of the nanoparticles with an excess of 2,3-dimercaptosuccinic acid (DMSA). Hereto 10 mg/ml of magnetic nanoparticles in toluene are mixed with 200 mg/ml of DMSA in DMSO for 48 hours. Black precipitates were observed, isolated through centrifugation and redispersed in water.

## 4 APPLICATIONS OF INORGANIC NANOPARTICLES

### 4.1 Metal nanoparticles for sensing

The LSPR properties of the nanoparticles depend on different parameters such as changes in the local environment of the nanostructure. The latter also means that when a biofunctionalized nanoparticle would bind an analyte of interest, the absorption properties of the nanoparticles will change due to changes of the refractive index of the close environment of the nanoparticles. This phenomenon could therefore be used for (bio)sensing applications using both nanoparticles in suspension (see 2.1) or arrays of nanoparticles attached to a transparent substrate (see 2.2).

Nanoparticles ~42 nm	$\lambda$ shift (nm)/ RI units
Au NP suspension	$91.7 \pm 1.9$
Au NP array	$64.7 \pm 7.1$

**Table 1:** Sensitivity of the nanoparticles in suspension and in array configuration towards changes in RI units.

In a first step, the sensitivity of the nanoparticles for changes in refractive index (RI) was assessed. Hereto, the nanoparticle suspensions and the nanoparticle films were measured in glycerol solutions with increasing RI. Since the LSPR band of the nanoparticles is sensitive to local RI changes, the absorption band of the nanoparticle in suspension or the nanoparticles in the films (ie. array configuration) shifted to higher absorption values and higher wavelengths (data not shown). By plotting these absorption and wavelengths shifts as a function of RI, linear calibration curves could be derived for the different nanoparticle films. The slope of these calibration curves are a measure for the sensitivity of the nanoparticles in suspension or in the nanoparticle films. Various sizes and materials were evaluated (data not shown). Both approaches (in suspension and in films) use gold

nanoparticles of ~42 nm and show a similar sensitivity towards changes in RI (Table 1).

In a second step, we performed biological sensing experiments using antibody/antigen interactions. For the biosensing experiments using nanoparticles in suspension, we investigated the response of nanoparticles functionalized with Protein A towards Human IgG binding. For this approach we used a double beam UV/Vis spectrophotometer (UV-1601PC of Shimadzu®) as a read-out device. Figure 3 shows the spectra after binding of various concentrations of Human IgG on the Protein A modified gold nanoparticles.

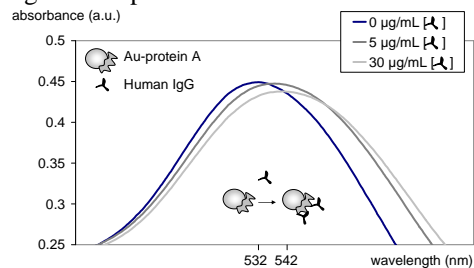


**Figure 3:** UV/Vis spectra of Protein A functionalized nanoparticles after binding Human IgG.

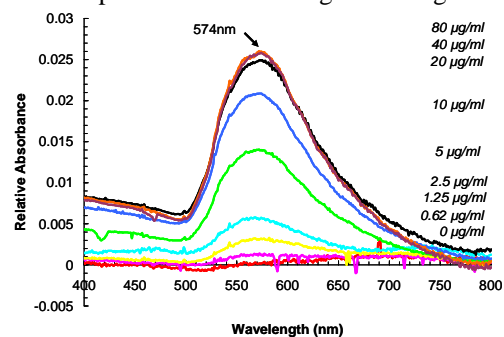


**Figure 4:** Difference absorption spectra of the binding of anti-biotin onto the biotin coated nanoparticle film.

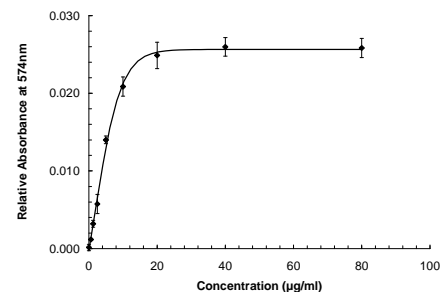


**Figure 5:** Dose response curves of the binding of anti-biotin onto the biotin coated nanoparticle film.

The alternative LSPR biosensing approach is based on the use of nanoparticle arrays as sensing substrate in the Transmission Plasmon Biosensor (TPB)(see 2.2). The advantage of this approach is that the films can be washed in between the different assay steps. We used the interaction of an antibody (anti-biotin) on a nanoparticle film coated with a small molecule (biotin) as a biological model system to evaluate the TPB. Figure 4 shows the difference absorption spectra of the binding of different

concentrations of antibody on a functionalized nanoparticle film (~42 nm). By plotting the difference absorbance at the maximum absorbance at 574 nm, we are able to subtract a dose response curve (Figure 5). A clear concentration dependent signal can be observed.

In the above-mentioned TPB experiments, a full-spectrum plate reader (Molecular Devices®) is used as a read-out for the nanoparticle films. In our group, we are currently investigating an alternative measurement set-up using a quadrant detector.

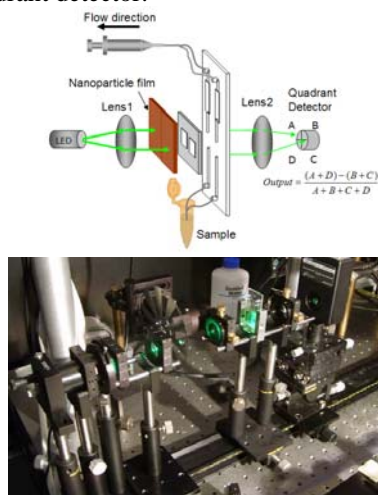


**Figure 6:** Schematic of the home-made TPB set-up.

Our home-made setup focuses a light beam from an LED onto a gold nanoparticle film that is divided into two areas, one for reference and the other for the specific coated sample. The transmission light from the two areas are detected simultaneously with a quadrant cell photodetector (Figure 6) and the difference signal,  $(A+D)-(B+C)/(A+B+C+D)$ , provides an accurate measurement of the specific adsorption of an analyte on to the sample area. A microfluidic chip is integrated with the nanoparticle film as well for the sample introduction

## 4.2 Metal nanoparticles for hyperthermia

Small spherical gold nanoparticles show a characteristic LSPR band around 530 nm. By increasing their size, the LSPR band will shift to higher wavelengths in the visible region of the electromagnetic spectrum. However, these visible light absorbing nanoparticles cannot be used for *in vivo* hyperthermia treatment. This application requires light in the spectral 650-900 nm region where the tissue has the highest transmissibility. By changing the nanoparticle shape from spherical to star shaped, one can tune the LSPR absorption wavelength from visible to near-infrared (NIR). These non-spherical nanoparticles absorb the NIR light followed by rapid conversion of this light into released heat. The ability of these nanoparticles to efficiently convert absorbed light into localized heat can be exploited for hyperthermia treatment of cancer.

Before the functionalized star shaped gold nanoparticle can be used in hyperthermia treatment, the heat generation properties of the various nanoparticles were characterized and compared with spherical nanoparticles using a home-made CW laser set-up (~633 nm) in combination with a thermocouple (Figure 7).

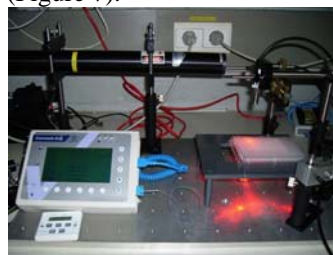


**Figure 7:** Laser set-up for nanoparticle heating.

Using this approach, we were able to demonstrate the rapid heating of the solution surrounding the star shaped nanoparticles when applying the laser in comparison with the test solution (data not shown).

## 4.3 Magnetic nanoparticles for imaging

Some of the recent successes in MRI rely on the use of nanomaterials, such as the biocompatible commercially available iron oxide nanoparticles. However, these iron oxide nanoparticles show a very low magnetic susceptibility (e.g. as compared to pure Fe) which makes them not the best choice for sensitive imaging. In our group, we focus on the synthesis and (bio)functionalization of magnetic nanoparticles of various high potential materials such as FePt. The FePt particles have a high magnetic moment and a higher susceptibility as compared to iron oxide particles and are more stable against oxidation than other common high moment magnetic particles such as Co or Fe.

## 5 CONCLUSIONS

In this paper, we describe several synthesis and surface modification methods to obtain stable gold and superparamagnetic Fe<sub>3</sub>O<sub>4</sub> or FePt nanoparticles. The properties of these nanoparticles were tuned and optimized for the needs defined by the application. Furthermore, we showed some preliminary experiments showing the high potential of these nanoparticles for biological applications including LSPR sensing, hyperthermia and imaging.

## REFERENCES

- [1] M. Seydack, *Biosens. Bioelect.*, 20, 2454-2469, 2005
- [2] G. Frens, *Nat. Phys. Sc.*, 241, 20, 1973.
- [3] E. Hao, R.C. Bailey, G.C. Schatz, J.T. Hupp, S. Li, *Nanoletters*, 4, 327-330, 2004
- [4] S. Sun, H. Zeng, D. Robinson, S. Raoux, P. Rice, S. Wang, G. Li, *JACS*, 126, 273-279, 2003
- [5] S. Sun, C. Murray, D. Weller, L. Folks, A. Moser, *Science*, 287, 1989-1992, 2000
- [6] S. Lin, Y. Tsai, C. Chen, C-Lin, C. Chen, *J. Phys. Chem. B*, 108, 2134-2139, 2003